

The physical mechanism of radio-quiet turn-on changing-look active galactic nuclei

SHUANG-LIANG LI¹ AND XINWU CAO²

¹*Shanghai Astronomical Observatory, Chinese Academy of Sciences, 80 Nandan Road, Shanghai 200030, People's Republic of China*

²*Institute for Astronomy, School of Physics, Zhejiang University, 866 Yuhangtang Road, Hangzhou 310058, People's Republic of China*

ABSTRACT

It is suggested that the variation of mass accretion rate in accretion disk may be responsible for the occurrence of most changing-look active galactic nuclei (CL AGNs). However, the viscous timescale of a thin disk is far longer than the observed timescale of CL AGNs. Though this problem can be resolved by introducing the large-scale magnetic field, the mechanism for radio-quiet CL AGNs with weak/absent large-scale magnetic field remains a mystery. In this work, we assume that the thin accretion disk is collapsed from the inner advection-dominated accretion flow (ADAF) instead of substituting by the outer thin disk through advection. This idea is tested by comparing the cooling timescale (t_{cool}) of an ADAF with the observed timescale (t_{tran}) of turn-on CL AGNs. We compile a sample of 102 turn-on CL AGNs from the archived data and calculate the cooling timescale of an ADAF with the critical mass accretion rate based on some conventional assumptions. It is found that t_{cool} is much shorter than t_{tran} in most of the CL AGNs, which validates our assumption though t_{cool} is not consistent with t_{tran} ($t_{\text{cool}} < t_{\text{tran}}$). However, this is reasonable since most of the CL AGNs were observed only two times, indicating that the observed timescale t_{tran} is the maximum value because the changing-look can indeed happen before the second observation.

Keywords: accretion, accretion disks – black hole physics – magnetic fields – active galactic nuclei

1. INTRODUCTION

Depending on whether the broad emission line region (BLR) is obscured by a torus, active galactic nuclei (AGNs) can be roughly classified into type 1 and type 2 based on the presence or absence of broad emission lines in the AGN unified model (e.g., Seyfert 1943; Antonucci 1993). Usually, the type of AGN will remain unchanged within the viscous timescale ($\sim 10^4 - 10^7$ years) of a thin accretion disk in AGNs (Shakura & Sunyaev 1973; Frank et al. 2002). However, some AGNs (several hundreds) have been observed to change their type in much shorter timescale ranging from several months to tens of years (e.g., Parker et al. 2016; Gezari et al. 2017; Yang et al. 2018; MacLeod et al. 2019; Wang et al. 2020; Green et al. 2022; Dong et al. 2024; Panda & Śniegowska 2024; Yang et al. 2025). These objects are named as changing-look AGNs (CL AGNs). Exploring the physics of CL AGNs can help us understand the accretion process in AGNs.

When CL AGNs are first discovered, people consider that the obscuration of torus on BLR should be responsible for the occurrence of CL AGNs (e.g., Goodrich 1989; Tran et al. 1992; Elitzur 2012). However, if this scenario is correct, the variability of infrared emissions should be very weak, inconsistent with the large amplitude variations in CL AGNs (Sheng et al. 2017). The low polarization of optical emissions in CL AGNs provides further evidence opposing the torus obscured model (Hutsemékers et al. 2019). The other popular model for CL AGNs is the change of global mass accretion rate in disk, which is the most promising mechanism so far and has been supported by the co-variation of multi-wavelength emissions (e.g., Ross et al. 2018; Śniegowska et al. 2020; Yang et al. 2023). However, as mentioned above, the viscous timescale ($t_{\text{vis}} \sim R/V_{\text{R}}$) of a thin disk is far longer than the observed timescale of CL AGNs. Obviously, by constraining the disk size R or/and enhancing the radial velocity V_{R} can help to solve

this inconsistency. Sniegowska et al. (2020) suggested that the instability of a narrow disk region between an inner advection-dominated accretion flows (ADAF) and an outer thin disk can qualitatively explain the CL AGNs with multi-CL (see also Pan et al. 2021). It is found that the radial velocity of a thin disk threaded by the large-scale poloidal magnetic field can be significantly improved for the reason that the outflow driven by the magnetic field can transfer a large fraction of the angular momentum of accretion disk. (e.g, Cao & Spruit 2013; Li & Begelman 2014; Feng et al. 2021; Wu & Gu 2023). In addition, the disk scale-height elevated by the large-scale toroidal field can also improve the radial velocity (e.g, Dexter & Begelman 2019). All these models can qualitatively fix the inconsistency between the observed timescale and the theoretical viscous timescale. However, most of the CL AGNs are radio-quiet, i.e., the large-scale magnetic field threading on the accretion disk should be very weak or absent. In this circumstance, the radial velocity of thin disk cannot be significantly improved, leading to the much longer viscous timescale of a thin disk than the typical observed timescale of CL AGNs. Therefore, another mechanism is necessary to explain the the observed timescale in radio-quiet CL AGNs.

On the other hand, the accretion physics of black hole should be scaled-free. It is well known that the accretion flow of low-hard state in black hole X-ray binaries is composed by an inner ADAF and an outer thin accretion disk, while the high-soft state is dominated by a thin disk only (e.g., Esin et al. 1997; Yuan & Narayan 2014). Some works argued that CL AGNs have analogous accretion structure with the state transition of black hole X-ray binaries, where the type 2 and type 1 of CL AGNs correspond to the low-hard and high-soft state of X-ray binaries, respectively (e.g., Ruan et al. 2019; Lyu et al. 2022). The reasons include the similar relationship between their UV-to-X-ray spectral index α_{OX} and the Eddington ratio λ and the similar critical Eddington ratio to separate the low/high state in X-ray binaries and that to separate the type 1/2 in CL AGNs. Inspired by this opinion, we consider the possibility that the inner ADAF collapses to a thin accretion disk through radiative cooling, instead of replacing by the outer thin disk through radial advection. This mechanism will resolve the problem that large-scale magnetic field may be very weak or absent in radio-quiet AGNs. In this work, we investigate the cooling timescale of an ADAF during the state transition and compare it with the observed timescale of turn-on CL AGNs.

2. MODEL

In the low-hard state of black hole X-ray binaries, the X-ray emissions consist of a strong power-law component plus a weak blackbody component, which is believed to come from an inner optically thin and geometrically thick ADAF and an outer optically thick and geometrically thin accretion disk, respectively (Remillard & McClintock 2006; Yuan & Narayan 2014). The radiative efficiency of an ADAF is roughly proportional to the square of mass accretion rate, resulting in the more efficient cooling rate than the heating rate when the Eddington ratio increases ($\eta \propto \dot{m}^2$, Narayan & Yi 1994, 1995). Therefore, an ADAF will collapse to a thin accretion disk and the binary system will enter the high-soft state at a critical Eddington ratio ($\lambda_{\text{Edd}} \gtrsim 0.01$).

The energy equation of an ADAF can be given as

$$q^+ = q^- + q_{\text{adv}} = q^- + f_{\text{adv}}q^+, \quad (1)$$

where q^+ , q^- , q_{adv} are the viscously heating rate, the cooling rate and the advected rate of energy, respectively. In a standard ADAF, $q^+ \gg q^-$, so f_{adv} is ~ 1 (Narayan & Yi 1994, 1995). However, the Coulomb coupling between electron and proton will become more and more efficiently as the Eddington ratio increases. When closing to a critical value, a large fraction of the released gravitational energy will be taken away through radiation, leading to the formation of a thin disk (Narayan & Yi 1995; Narayan et al. 1998).

As Narayan & Yi (1995), the cooling timescale of an ADAF can be written as

$$t_{\text{cool}} \sim \frac{u}{q^-}, \quad (2)$$

where $u \sim 3n_i kT_i/2 \sim 3P/2$ is the internal energy of gas, and $P \cong P_i$ is the pressure of gas. The viscous dissipation rate of energy q^+ is

$$q^+ = -\alpha PR \frac{d\Omega}{dR} \cong \frac{3}{2} f_{\Omega} \alpha P \Omega_K, \quad (3)$$

where α is the dimensionless viscosity parameter. Parameter f_{Ω} is given by $f_{\Omega} = \Omega/\Omega_K$, where Ω and Ω_K are the angular velocity and the Keplerian angular velocity of the gas, respectively. Combining with equations (1) and (3), equation (2) can be rewritten as

$$t_{\text{cool}} = \frac{1}{(1 - f_{\text{adv}}) f_{\Omega} \alpha \Omega_K}. \quad (4)$$

As mentioned above, the advected rate of energy ($q_{\text{adv}} = f_{\text{adv}}q^+$) will decrease with increasing Eddington ratio. However, the detailed value of f_{adv} is unclear, which will vary with the viscosity parameter α and the ratio of gas pressure to the magnetic pressure β (Narayan & Yi 1995; Narayan et al. 1998). In this work, we adopt a typical value of $f_{\text{adv}} \sim 0.3$ when the critical mass accretion rate \dot{m}_{crit} is adopted, where \dot{m}_{crit} is given as $\dot{m}_{\text{crit}} \cong \alpha^2$ in theory (see e.g., Narayan & Yi 1995). The angular velocity of a thin accretion disk is usually adopted to be Keplerian because its disk temperature is low. However, the temperature of an ADAF is very high (the ion temperature can be close to the virial temperature) since most of the released gravitational energy is stored in the gas instead of being radiated away. The higher temperature will produce a strong pressure gradient force, which offsets part of the gravitational force and leads to a sub-Keplerian angular velocity (see e.g., Narayan & Yi 1994, 1995). Therefore, the angular velocity of an ADAF before collapsing to a thin disk is sub-Keplerian. However, the angular velocity will increase with the decrease of temperature when the mass accretion rate is close to the critical mass accretion rate. So we adopt 90% of the Keplerian velocity ($f_{\Omega} = 0.9$) in this work. Our results will be qualitatively the same even a fully Keplerian velocity as in a thin disk is adopted (resulting in a t_{cool} value 10% smaller).

The critical mass accretion rate \dot{m}_{crit} ($= \dot{M}_{\text{crit}}/\dot{M}_{\text{Edd}}$) is equal to λ_{crit} assuming a conventional radiation efficiency $\eta = 0.1$, where $\dot{M}_{\text{Edd}} = L_{\text{Edd}}/0.1c^2$ is the Eddington accretion rate. However, the detailed value of \dot{m}_{crit} in CL AGNs are unknown because most of objects only have two spectroscopic observations, i.e., one faint state and one bright state, respectively. Therefore, we adopt the value of Eddington ratio λ_{Edd} at bright state as \dot{m}_{crit} (see column 3 in table 1). In addition, the bolometric luminosity of CL AGNs in our sample is estimated with the continuum flux at 5100\AA , indicating the temperature at the transition radius R_{tr} between the inner ADAF and outer thin disk should be larger than the temperature corresponding with wavelength 5100\AA ($\sim 5700\text{K}$). Therefore, R_{tr} can be estimated by solving the following equation:

$$\sigma T_{\text{eff}}^4 = \frac{3GM_{\text{bh}}\dot{M}}{8\pi R^3} \left(1 - \sqrt{\frac{6R_{\text{g}}}{R}} \right), \quad (5)$$

where σ , G , and $R_{\text{g}} = GM_{\text{bh}}/c^2$ are the Stefan-Boltzmann constant, the gravitational constant and the gravitational radius, respectively. With f_{adv} , f_{Ω} , α , and the transition radius R_{tr} , the cooling timescale of an ADAF at R_{tr} can be gotten with equation (4).

3. SAMPLE

Most of CL AGNs discovered in early years are identified as turn-off CL AGNs because they are usually picked up firstly from the spectroscopically-confirmed quasars (Yang et al. 2025). It is hard to find a relatively large turn-on CL AGN sample until this year. In order to compare with the theoretical model, the black hole mass, Eddington ratio and timescale of CL AGNs are all required (see Section 4 for details). We compile a sample of 102 turn-on CL AGNs by searching the archived data in this work (see table 1). Most of the objects (82) are picked up from Yang et al. (2025), while other 12 and the last 8 objects are selected from Panda & Śniegowska (2024) and Dong et al. (2024), respectively. To ensure the formal consistency, we rewrite all the objects as SDSSJXXXX+/-XXXX in column (1). The black hole mass m_{bh} in column (3) are all estimated with the width of broad emission lines (Vestergaard & Peterson 2006). Column (4) gives the Eddington ratio λ_{Edd} of bright states in CL AGNs. Column (5) and (6) represent the observed modified Julian dates of faint state and bright state, respectively. The transition timescale t_{tran} in column (7) and cooling timescale t_{cool} in column (9) indicate the observed timescale of CL AGNs and the cooling timescale of ADAF given by theory, respectively. t_{tran} has been corrected to the value in rest frame of the object ($t_{\text{tran}} = (\text{MJD}_2 - \text{MJD}_1)/(1+z)$, where z is the redshift).

Table 1. The sample.

Name	z	m_{bh}	λ_{Edd}	MJD ₁	MJD ₂	t_{tran}	Ref.	t_{cool}	Name	z	m_{bh}	λ_{Edd}	MJD ₁	MJD ₂	t_{tran}	Ref.	t_{cool}
(1)	(2)	(3)	(4)	(5)	(6)	(7)	(8)	(9)	(1)	(2)	(3)	(4)	(5)	(6)	(7)	(8)	(9)
SDSSJ0002+0027	0.291	8.94±0.02	-1.99	52559	55477	2260	1	2764±63	SDSSJ0023+0035	0.422	9.17±0.04	-1.61	51816	55480	2577	1	3507±162
SDSSJ0040+1609	0.294	7.85±0.04	-1.49	51884	60181	6412	2	813±38	SDSSJ0047+1541	0.031	7.07±0.21	-2.22	51879	59856	7734	2	322±87
SDSSJ0107+2428	0.160	8.37±0.05	-2.07	57367	59970	2244	2	1479±85	SDSSJ0110+0026	0.019	7.09±0.03	-2.12	51794	59880	7937	2	329±11
SDSSJ0132+1501	0.170	8.15±0.02	-2.21	51884	60240	7142	2	1101±25	SDSSJ0141+0105	0.101	8.39±0.08	-2.07	51788	58794	6363	2	1512±142
SDSSJ0144+3140	0.124	7.66±0.03	-1.48	57725	58133	363	3	663±23	SDSSJ0146+1311	0.160	8.10±0.02	-2.07	51820	60196	7221	2	1092±25
SDSSJ0225+0030	0.504	9.27±0.09	-2.15	55445	55827	254	1	4112±431	SDSSJ0334+0051	0.429	8.39±0.05	-1.65	52178	60193	5609	2	1489±86
SDSSJ0803+2207	0.125	7.59±0.02	-1.72	52943	60322	6559	2	595±14	SDSSJ0813+4608	0.054	7.37±0.02	-1.53	51877	60322	8014	2	477±11
SDSSJ0819+3019	0.098	7.98±0.01	-1.65	52619	60239	6943	2	937±11	SDSSJ0823+4202	0.126	7.56±0.06	-1.65	52266	60016	6883	2	583±41
SDSSJ0829+2319	0.144	8.09±0.01	-2.69	53349	60323	6096	2	934±11	SDSSJ0829+4154	0.126	8.71±0.02	-2.07	52266	54524	2005	1	2162±50
SDSSJ0831+3646	0.195	8.26±0.09	-1.74	52312	57367	4230	3	1335±142	SDSSJ0837+0356	0.064	7.13±0.05	-2.07	52646	59288	6245	2	365±21
SDSSJ0838+3719	0.211	8.72±0.04	-1.77	52320	59200	5681	3	2160±98	SDSSJ0853+2128	0.084	7.83±0.03	-1.56	53680	59078	4979	3	776±27
SDSSJ0854+1113	0.167	8.04±0.09	-1.76	54084	58794	4036	2	1017±109	SDSSJ0901+2907	0.218	8.71±0.02	-2.59	56341	60239	3200	2	2094±45
SDSSJ0906+4046	0.167	8.07±0.05	-2.85	52668	60323	6560	2	944±53	SDSSJ0908+0755	0.144	8.68±0.02	-2.93	52973	60240	6352	2	2245±48
SDSSJ0910+1907	0.188	7.87±0.03	-1.91	53700	60029	5327	2	832±29	SDSSJ0914+0502	0.143	8.49±0.08	-2.92	52652	58879	5448	2	1844±169
SDSSJ0915+4814	0.101	8.07±0.02	-2.71	52637	59501	6234	2	1114±26	SDSSJ0926-0006	0.201	6.95±0.04	-1.11	52000	59227	6017	2	293±14
SDSSJ0936+2726	0.103	6.68±0.02	-0.79	53385	59527	5568	2	218±5	SDSSJ0937+2602	0.162	7.58±0.02	-1.19	53733	57369	3129	3	612±14
SDSSJ0947+5449	0.620	8.35±0.10	-1.09	56011	58794	1718	2	1471±176	SDSSJ0951+3416	0.132	7.85±0.01	-1.74	53388	60240	6053	2	840±10
SDSSJ0952+2229	0.081	6.44±0.06	-1.28	53734	60322	6094	2	163±12	SDSSJ0955+1037	0.284	8.39±0.04	-0.93	52996	59200	4832	3	1529±71
SDSSJ1000+0354	0.125	7.26±0.11	-1.22	52289	59333	5798	2	428±57	SDSSJ1002+0303	0.023	7.18±0.03	-1.79	52235	59250	6855	2	371±13
SDSSJ1003+0202	0.215	7.74±0.41	-2.53	52235	58494	5564	2	763±444	SDSSJ1003+0458	0.124	8.02±0.14	-2.55	52325	58495	5489	2	1019±172
SDSSJ1003+3525	0.119	8.28±0.05	-2.01	53389	58612	4668	2	1291±74	SDSSJ1003+1932	0.467	8.84±0.03	-1.58	53762	57817	2764	1	2514±84
SDSSJ1009+3539	0.110	8.35±0.07	-2.17	53389	58896	4961	2	1446±118	SDSSJ1011+5442	0.247	7.63±0.01	-0.79	57073	60291	2581	2	645±7
SDSSJ1012+5559	0.126	7.71±0.11	-1.61	52407	58163	5112	2	679±90	SDSSJ1017+0658	0.045	7.63±0.11	-2.19	55679	58843	3027	2	628±83
SDSSJ1020+2437	0.189	9.13±0.01	-2.39	53734	60240	5472	2	3523±37	SDSSJ1058+6338	0.202	7.42±0.05	-1.39	54498	60059	4626	2	505±30
SDSSJ1102+5722	0.142	8.21±0.05	-2.24	52427	60012	6642	2	1137±66	SDSSJ1105+0516	0.091	7.67±0.08	-1.86	52353	59231	6303	2	645±61
SDSSJ1110+0804	0.116	7.51±0.17	-2.48	52723	58136	4850	2	520±110	SDSSJ1111+1401	0.110	7.48±0.07	-1.55	53377	58612	4716	2	528±44
SDSSJ1115+0544	0.090	7.63±0.06	-1.61	52326	57393	4649	2	620±44	SDSSJ1126+0510	0.170	8.22±0.04	-2.29	52376	60059	6567	2	1239±57
SDSSJ1132+0357	0.091	7.57±0.04	-1.80	52642	58612	5472	2	571±26	SDSSJ1136+4450	0.116	8.30±0.02	-1.47	53083	57732	4166	1	1385±31
SDSSJ1149+3351	0.081	8.12±0.02	-2.18	53491	60052	6070	2	1104±25	SDSSJ1155+0048	0.209	9.21±0.01	-2.82	51662	59317	6332	2	3430±36
SDSSJ1158+1003	0.070	7.47±0.05	-3.38	52733	58844	5712	2	515±29	SDSSJ1159+0513	0.059	7.73±0.01	-1.71	52375	60319	7499	2	706±8
SDSSJ1159+6545	0.122	8.56±0.07	-2.08	52316	58496	5508	2	1807±147	SDSSJ1205+3335	0.299	8.22±0.02	-1.06	56418	58467	1577	3	1227±28
SDSSJ1226+4559	0.109	7.87±0.07	-2.81	52821	60013	6485	2	792±64	SDSSJ1231+3232	0.065	7.76±0.02	-1.71	53472	60013	6139	2	730±17
SDSSJ1239+0739	0.133	7.48±0.09	-1.87	53474	60060	5813	2	514±55	SDSSJ1311+0705	0.301	7.79±0.19	-1.38	54507	59295	3680	2	778±1203
SDSSJ1311+4300	0.285	7.91±0.15	-1.44	57783	60013	1735	2	874±162	SDSSJ1327+4025	0.078	7.75±0.06	-2.75	53091	59250	5715	2	743±52
SDSSJ1328+6227	0.091	7.81±0.04	-2.63	52339	58197	5371	2	733±33	SDSSJ1340+4006	0.171	8.22±0.02	-1.89	53050	59729	5704	2	1264±29
SDSSJ1341-0049	0.175	7.31±0.25	-1.40	51671	58256	5604	2	441±145	SDSSJ1413+5305	0.456	8.38±0.03	-0.62	52762	58289	3796	1	1506±52
SDSSJ1433+4943	0.125	7.97±0.13	-2.36	52460	59317	6095	2	861±136	SDSSJ1442+5558	0.077	7.24±0.03	-1.36	52668	59727	6554	2	406±14
SDSSJ1511+2101	0.081	8.15±0.03	-1.40	54525	59732	4819	3	1142±39	SDSSJ1524+4327	0.198	8.34±0.05	-2.41	52468	58987	5442	2	1433±83
SDSSJ1538+4607	0.203	8.49±0.03	-2.63	52781	60195	6163	2	1565±52	SDSSJ1552+2102	0.172	7.91±0.02	-1.51	53557	60193	5662	2	850±19
SDSSJ1611+1642	0.155	8.15±0.01	-1.89	53555	60206	5758	2	1168±13	SDSSJ1612+3113	0.177	8.95±0.02	-3.16	58244	60107	1583	2	2280±44
SDSSJ1612+3816	0.199	8.05±0.03	-2.22	53146	60117	5814	2	973±34	SDSSJ1636+3930	0.182	7.60±0.08	-1.52	52381	60206	6620	2	626±60
SDSSJ1638+4712	0.114	7.97±0.04	-2.32	52144	59726	6806	2	904±41	SDSSJ1640+2819	0.181	7.93±0.05	-2.05	53472	59724	5294	2	923±53
SDSSJ1642+4423	0.227	7.97±0.04	-1.58	53557	60193	5408	2	943±43	SDSSJ1643+5000	0.060	7.39±0.03	-2.47	57187	60206	2848	2	460±16
SDSSJ1652+3416	0.263	8.18±0.05	-1.93	52435	59314	5447	2	1152±67	SDSSJ1723+5504	0.295	8.80±0.15	-1.73	51813	51997	142	1	2300±420
SDSSJ2120-0056	0.251	8.38±0.03	-2.02	52932	60181	5795	2	1428±49	SDSSJ2150-0106	0.088	7.45±0.08	-2.10	53172	58794	5168	2	507±48
SDSSJ2156+2907	0.092	7.49±0.10	-1.52	56101	59879	3460	2	553±66	SDSSJ2159+0556	0.111	8.15±0.02	-2.81	58431	60197	1590	2	1081±25
SDSSJ2201+0352	0.136	7.60±0.07	-2.05	58429	60197	1556	2	636±52	SDSSJ2203+1124	0.186	6.82±0.09	-1.29	52224	58105	4959	2	249±27
SDSSJ2225+2019	0.155	8.18±0.03	-2.72	56189	60197	3470	2	1245±42	SDSSJ2146+0009	0.621	9.44±0.02	-2.21	52968	55478	1548	1	4618±95
SDSSJ2241-0121	0.058	8.31±0.03	-2.23	55824	57724	1796	1	1288±44	SDSSJ2252+0109	0.534	8.83±0.03	-1.42	52178	55500	2166	1	2528±87
SDSSJ2320+1448	0.082	7.60±0.04	-2.36	52258	59501	6693	2	569±26	SDSSJ2336+1514	0.147	7.73±0.02	-1.48	52234	59821	6615	2	718±16
SDSSJ2346+0109	0.509	9.00±0.19	-1.64	52524	57684	3419	1	2986±708	SDSSJ2348+0741	0.464	7.87±0.06	-1.34	56164	60240	2784	2	850±60

Notes: Col. (1): Source name. Col. (2): Redshift. Col. (3): Black hole mass $m_{\text{bh}} = \log(M_{\text{BH}}/M_{\odot})$, where M_{BH} and M_{\odot} are the black hole mass and solar mass, respectively. Col. (4): Eddington ratio of CL AGNs in bright state. Col. (5): modified Julian date of faint state. Col. (6): modified Julian date of bright state. Col. (7): Observational timescale for CL AGNs. Col. (8): References. Col. (9): Cooling timescale in theory with uncertainty derived from the uncertainty of black hole mass.

References. 1, Panda & Śniegowska (2024); 2, Yang et al. (2025); 3, Dong et al. (2024).

4. RESULTS

We compare the observed timescale t_{tran} of CL AGNs and the cooling timescale t_{cool} of an ADAF in Figure 1, where the red solid line represents $t_{\text{tran}} = t_{\text{cool}}$. It is found that t_{cool} is much shorter than t_{tran} in most of CL AGNs, while $t_{\text{cool}} \gg t_{\text{tran}}$ is found in two CL AGNs, i.e., SDSSJ0225+0030 and SDSSJ1723+5504. This result confirms our assumption that the inner ADAF can collapse to a thin disk within the observed timescale of turn-on CL AGNs. The origin for the two special objects with $t_{\text{cool}} \gg t_{\text{tran}}$ may be related with the large-scale magnetic field (see section 5 for details).

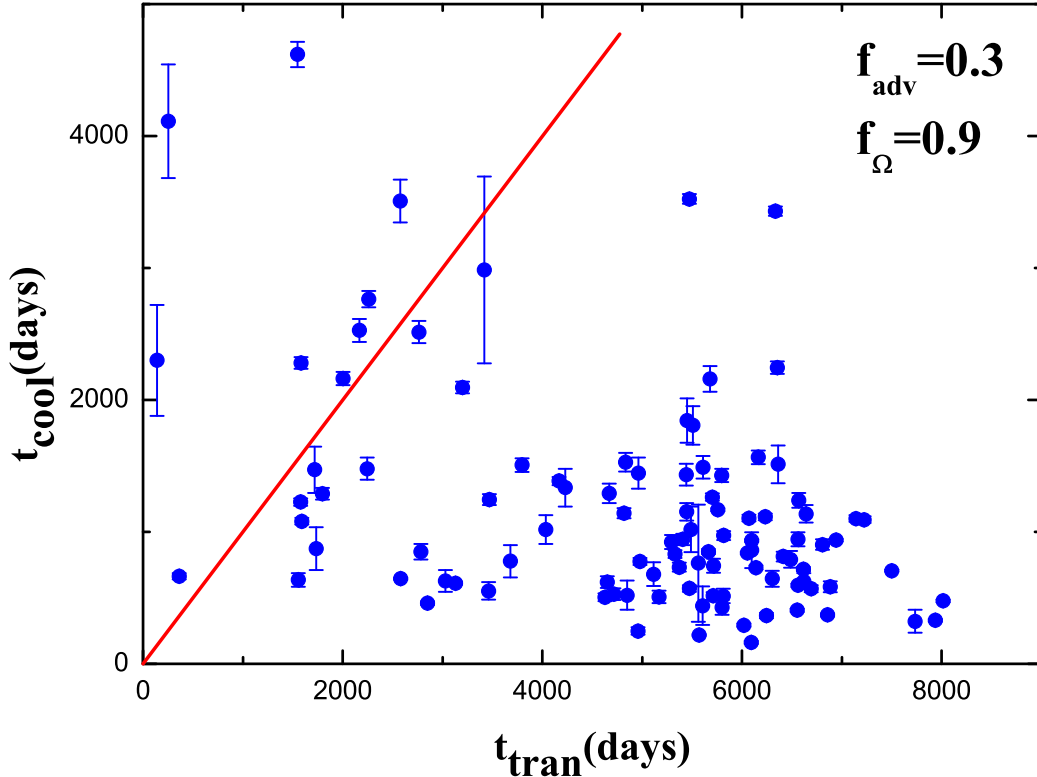


Figure 1. Comparison of the observed timescale t_{tran} of CL AGNs with the cooling timescale t_{cool} of an ADAF, where the solid red line represent $t_{\text{tran}} = t_{\text{cool}}$.

5. SUMMARY AND DISCUSSION

For most of radio-quiet CL AGNs where the large-scale magnetic field is absent or very weak, the viscous timescale of a thin disk would be too long compared with the observed timescale. Therefore, it is possible that, instead of being replaced by the outer thin disk, the formation of inner thin disk can be collapsed from the inner ADAF in CL AGNs. We compile a sample of 102 turn-on CL AGNs from the archived data to test this idea in this work. It is found that the cooling timescale t_{cool} of an ADAF is shorter than the observed timescale t_{tran} of most turn-on CL AGNs, supporting our assumption though they are not consistent in most of objects. This inconsistency between t_{cool} and t_{tran} may originate from: 1) the observed timescale t_{tran} is the upper limit instead of detailed value because the bright state in most of CL AGNs is observed one time only. Even the light-curves in these objects are available, however, the variation of Eddington ratio during the transition is very small. People can't detect obvious flares from the light-curves (see e.g., Yang et al. 2025). CL AGNs can be identify only from the dis/appearance of broad emission lines through spectroscopic observations; 2) adopting the Eddington ratio at bright state as the critical mass accretion rate is also an upper limit, resulting on a larger viscosity parameter α and smaller t_{cool} . Furthermore, it is found that a large fraction of objects picked up from Panda & Śniegowska (2024) have more than two spectroscopic data. So we compare t_{cool} with t_{tran} individually for the objects selected from Panda & Śniegowska (2024) and find the result is much better for this subsample (see Figure 2). Therefore, the main caveat of this manuscript is that most of the objects only have two spectral observations, leading to a much longer observed timescales (t_{tran}) than the actual timescales of CL. If better spectral data can be gathered by shortening observation intervals and increasing the number of observations in the future, we can measure t_{tran} more accurately and further test our model in this manuscript.

Different with most other objects, SDSSJ0225+0030 and SDSSJ1723+5504 have much shorter observed timescales, which may be due to the presence of large-scale magnetic field. The large-scale magnetic field threading on the outer thin accretion disk can launch strong outflows and take away the angular momentum of the disk, leading to a much faster radial velocity (see, e.g., Cao & Spruit 2013; Li & Begelman 2014). Therefore, the inner ADAF may be dragged inwards to the central black hole before it is totally cooling to a thin disk.

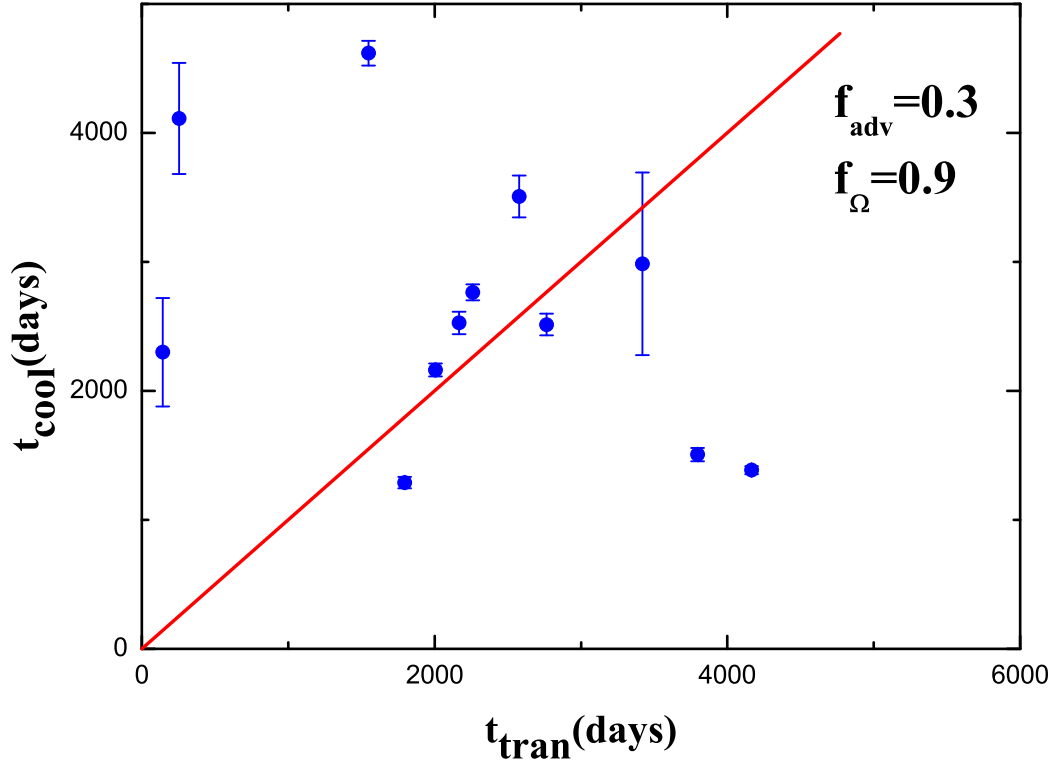


Figure 2. Same as figure 1, but for the objects picked up from Panda & Śniegowska (2024) only.

We investigate the cooling timescale of an ADAF and compare it with the turn-on CL AGNs only in this work. For turn-on CL AGNs, we can only focus on the collapse of an ADAF and the formation of a thin disk through radiative cooling. While for AGNs in bright state, the accretion process can be well described by a disk-corona model (Lusso & Risaliti 2017; Qiao & Liu 2018), where the optical-UV flux is emitted from a thin accretion disk and the hard X-ray flux comes from the inverse Compton scattering of optical-UV photons by the hot corona above the thin disk. When CL AGNs are turn-off, we have to consider simultaneously both the process of gas evaporation in thin disk and the process of gas condensation in corona, while these physical processes are still unclear so far. We will further explore this issue in future.

ACKNOWLEDGEMENTS

We thank the reviewer for his/her valuable comments, which help to clarify this manuscript. SLL thank Qian Yang for useful comments and sharing their data before official publication. This work is supported by the National Key R&D Program of China No. 2023YFA1607903, the NSFC (grants 12273089, 12073023, 12233007, 12361131579, 12347103), and the science research grants from the China Manned Space Project with No. CMSCSST-2021-A06, and the Fundamental Research Fund for Chinese Central Universities.

REFERENCES

- Antonucci, R. 1993, *Annual Review of Astronomy and Astrophysics*, 31, 473, doi: [10.1146/annurev.aa.31.090193.002353](https://doi.org/10.1146/annurev.aa.31.090193.002353)
- Cao, X., & Spruit, H. C. 2013, *ApJ*, 765, 149, doi: [10.1088/0004-637X/765/2/149](https://doi.org/10.1088/0004-637X/765/2/149)
- Dexter, J., & Begelman, M. C. 2019, *MNRAS*, 483, L17, doi: [10.1093/mnrasl/sly213](https://doi.org/10.1093/mnrasl/sly213)
- Dong, Q., Zhang, Z.-X., Gu, W.-M., Sun, M., & Zheng, Y.-G. 2024, arXiv e-prints, arXiv:2408.07335, doi: [10.48550/arXiv.2408.07335](https://doi.org/10.48550/arXiv.2408.07335)
- Elitzur, M. 2012, *The Astrophysical Journal Letters*, 747, L33, doi: [10.1088/2041-8205/747/2/L33](https://doi.org/10.1088/2041-8205/747/2/L33)
- Esin, A. A., McClintock, J. E., & Narayan, R. 1997, *ApJ*, 489, 865, doi: [10.1086/304829](https://doi.org/10.1086/304829)

- Feng, J., Cao, X., Li, J.-w., & Gu, W.-M. 2021, *ApJ*, 916, 61, doi: [10.3847/1538-4357/ac07a6](https://doi.org/10.3847/1538-4357/ac07a6)
- Frank, J., King, A., & Raine, D. J. 2002, *Accretion Power in Astrophysics: Third Edition*
- Gezari, S., Hung, T., Cenko, S. B., et al. 2017, *The Astrophysical Journal*, 835, 144, doi: [10.3847/1538-4357/835/2/144](https://doi.org/10.3847/1538-4357/835/2/144)
- Goodrich, R. W. 1989, *The Astrophysical Journal*, 342, 224, doi: [10.1086/167586](https://doi.org/10.1086/167586)
- Green, P. J., Pulgarin-Duque, L., Anderson, S. F., et al. 2022, *ApJ*, 933, 180, doi: [10.3847/1538-4357/ac743f](https://doi.org/10.3847/1538-4357/ac743f)
- Hutsemékers, D., González, B. A., Marin, F., et al. 2019, *A&A*, 625, A54, doi: [10.1051/0004-6361/201834633](https://doi.org/10.1051/0004-6361/201834633)
- Li, S.-L., & Begelman, M. C. 2014, *ApJ*, 786, 6, doi: [10.1088/0004-637X/786/1/6](https://doi.org/10.1088/0004-637X/786/1/6)
- Lusso, E., & Risaliti, G. 2017, *A&A*, 602, A79, doi: [10.1051/0004-6361/201630079](https://doi.org/10.1051/0004-6361/201630079)
- Lyu, B., Wu, Q., Yan, Z., Yu, W., & Liu, H. 2022, *ApJ*, 927, 227, doi: [10.3847/1538-4357/ac5256](https://doi.org/10.3847/1538-4357/ac5256)
- MacLeod, C. L., Green, P. J., Anderson, S. F., et al. 2019, *The Astrophysical Journal*, 874, 8, doi: [10.3847/1538-4357/ab05e2](https://doi.org/10.3847/1538-4357/ab05e2)
- Narayan, R., Mahadevan, R., & Quataert, E. 1998, in *Theory of Black Hole Accretion Disks*, ed. M. A. Abramowicz, G. Björnsson, & J. E. Pringle, 148–182, doi: [10.48550/arXiv.astro-ph/9803141](https://doi.org/10.48550/arXiv.astro-ph/9803141)
- Narayan, R., & Yi, I. 1994, *ApJL*, 428, L13, doi: [10.1086/187381](https://doi.org/10.1086/187381)
- . 1995, *ApJ*, 452, 710, doi: [10.1086/176343](https://doi.org/10.1086/176343)
- Pan, X., Li, S.-L., & Cao, X. 2021, *ApJ*, 910, 97, doi: [10.3847/1538-4357/abe766](https://doi.org/10.3847/1538-4357/abe766)
- Panda, S., & Śniegowska, M. 2024, *ApJS*, 272, 13, doi: [10.3847/1538-4365/ad344f](https://doi.org/10.3847/1538-4365/ad344f)
- Parker, M. L., Komossa, S., Kollatschny, W., et al. 2016, *Monthly Notices of the Royal Astronomical Society*, 461, 1927, doi: [10.1093/mnras/stw1449](https://doi.org/10.1093/mnras/stw1449)
- Qiao, E., & Liu, B. F. 2018, *MNRAS*, 477, 210, doi: [10.1093/mnras/sty652](https://doi.org/10.1093/mnras/sty652)
- Remillard, R. A., & McClintock, J. E. 2006, *ARA&A*, 44, 49, doi: [10.1146/annurev.astro.44.051905.092532](https://doi.org/10.1146/annurev.astro.44.051905.092532)
- Ross, N. P., Ford, K. E. S., Graham, M., et al. 2018, *Monthly Notices of the Royal Astronomical Society*, 480, 4468, doi: [10.1093/mnras/sty2002](https://doi.org/10.1093/mnras/sty2002)
- Ruan, J. J., Anderson, S. F., Eracleous, M., et al. 2019, *ApJ*, 883, 76, doi: [10.3847/1538-4357/ab3c1a](https://doi.org/10.3847/1538-4357/ab3c1a)
- Seyfert, C. K. 1943, *The Astrophysical Journal*, 97, 28, doi: [10.1086/144488](https://doi.org/10.1086/144488)
- Shakura, N. I., & Sunyaev, R. A. 1973, *A&A*, 500, 33
- Sheng, Z., Wang, T., Jiang, N., et al. 2017, *ApJL*, 846, L7, doi: [10.3847/2041-8213/aa85de](https://doi.org/10.3847/2041-8213/aa85de)
- Śniegowska, M., Czerny, B., Bon, E., & Bon, N. 2020, *A&A*, 641, A167, doi: [10.1051/0004-6361/202038575](https://doi.org/10.1051/0004-6361/202038575)
- Tran, H. D., Osterbrock, D. E., & Martel, A. 1992, *The Astronomical Journal*, 104, 2072, doi: [10.1086/116382](https://doi.org/10.1086/116382)
- Vestergaard, M., & Peterson, B. M. 2006, *ApJ*, 641, 689, doi: [10.1086/500572](https://doi.org/10.1086/500572)
- Wang, J., Xu, D. W., & Wei, J. Y. 2020, *ApJ*, 901, 1, doi: [10.3847/1538-4357/abaa48](https://doi.org/10.3847/1538-4357/abaa48)
- Wu, W.-B., & Gu, W.-M. 2023, *ApJ*, 958, 146, doi: [10.3847/1538-4357/acf839](https://doi.org/10.3847/1538-4357/acf839)
- Yang, Q., Green, P. J., Wu, X.-B., et al. 2025, *ApJ*, 980, 91, doi: [10.3847/1538-4357/ad94ed](https://doi.org/10.3847/1538-4357/ad94ed)
- Yang, Q., Wu, X.-B., Fan, X., et al. 2018, *The Astrophysical Journal*, 862, 109, doi: [10.3847/1538-4357/aaca3a](https://doi.org/10.3847/1538-4357/aaca3a)
- Yang, Q., Green, P. J., MacLeod, C. L., et al. 2023, *ApJ*, 953, 61, doi: [10.3847/1538-4357/acdedd](https://doi.org/10.3847/1538-4357/acdedd)
- Yuan, F., & Narayan, R. 2014, *ARA&A*, 52, 529, doi: [10.1146/annurev-astro-082812-141003](https://doi.org/10.1146/annurev-astro-082812-141003)